Wearable Transcutaneous CO_2 Monitor Based on Miniaturized Nondispersive Infrared Sensor

Vishal Varun Tipparaju, **Sabrina Jimena Mora**, **Jingjing Yu**, **Francis Tsow**, **Xiaojun Xian**[*]

Center for Bioelectronics and Biosensors, The Biodesign Institute, Arizona State University, Tempe, AZ 85287 USA.

Abstract

Transcutaneous oxygen and carbon dioxide provide the status of pulmonary gas exchange and are of importance in diagnosis and management of respiratory diseases. Though significant progress has been made in oximetry, not much has been explored in developing wearable technologies for continuous monitoring of transcutaneous carbon dioxide. This research reports the development of a truly wearable sensor for continuous monitoring of transcutaneous carbon dioxide using miniaturized nondispersive infrared sensor augmented by hydrophobic membrane to address the humidity interference. The wearable transcutaneous CO_2 monitor shows well-behaved response curve to humid CO_2 with linear response to CO_2 concentration. The profile of transcutaneous CO_2 monitored by the wearable device correlates well with the end-tidal CO_2 trend in human test. The feasibility of the wearable device for passive and unobstructed tracking of transcutaneous CO_2 in free-living conditions has also been demonstrated in field test. The wearable transcutaneous CO_2 monitoring technology developed in this research can be widely used in remote assessment of pulmonary gas exchange efficiency for patients with respiratory diseases, such as COVID-19, sleep apnea, and chronic obstructive pulmonary disease (COPD).

Keywords

I. Introduction

Arterial Blood Gases (ABG) carry important health information about the pulmonary gas exchange and have been commonly used in intensive care as a diagnostic tool to assess functions of cardio-respiratory system in patients. [1] The ABG test evaluates the blood oxygenation and acid-base balance by measuring the partial pressures of oxygen (PaO_2), carbon dioxide ($PaCO_2$), and pH in arterial blood. [2] Though being considered as the "gold standard", arterial blood gas test is invasive, limited to central laboratory settings, and unable to provide continuous measurement. Transcutaneous blood gas monitoring is a

[*]Corresponding Author: Xiaojun Xian, xiaojun.xian@asu.edu.

continuous and noninvasive technique for arterial blood gas determination, [3], [4]. It has been increasingly used in oxygen therapy management, [5] fetal monitoring, [6] and clinical physiology monitoring. [7] Besides the application in the intensive care, transcutaneous blood gas analysis has been increasingly adopted in routine clinical practice, [8], [9] and used in monitoring sleep apnea and other related disorders. [10]–[13] With the rapid spread of COVID-19 across the world, the demand for measuring transcutaneous blood gas has increased due to the occurrence of arterial hypoxemia as part of this disease. [14]–[16]

Though the non-invasive transcutaneous blood gas analysis is well established, it has been mostly confined to bench-top clinical devices. A miniaturized wearable device that can be simply attached to a patient's body for continuous monitoring of transcutaneous blood oxygen and carbon dioxide in a remote manner will revolutionize the healthcare for respiratory diseases, such as COVID-19, sleep apnea and chronic obstructive pulmonary disease (COPD). [15] In recent years, pulse oximetry has been miniaturized into wearable devices using optical sensing technologies for continuously monitoring of blood oxygen saturation (SpO$_2$), and is a commonly accepted method to indicate arterial blood oxygen concentration. [17]–[21] But not much has been explored to develop wearable devices for continuous monitoring of transcutaneous blood carbon dioxide.

The traditional transcutaneous CO$_2$ monitors (prices around a few thousand dollars) use electrochemical sensors (usually a variant of Stow-Severinghaus electrodes) to measure the transcutaneous partial pressure of CO$_2$ (PtcCO$_2$). [22], [23]. This kind of sensors determine the CO$_2$ partial pressure through measuring the pH of the electrolyte layer. This change in pH has a logarithmic relationship with the transcutaneous partial pressure of CO$_2$. But these electrochemical sensors are delicate, tend to drift over time, and require constant calibration and replacement of membrane[8] To avoid these drawbacks, various optical methods for PtcCO$_2$ monitoring have been reported. [24]–[26] But these optical sensors usually consist of bulky and complex components such as lamp, fiber optics, or reaction chamber, making them not compatible with miniaturized wearable platform. Moreover, traditional transcutaneous CO$_2$ monitors heat up the area of skin where the sensor patches are placed to improve the visibility and diffusion of CO$_2$ in the contact area. This procedure is known to be painful since it damages the skin and the associated tissue underneath in long-term monitoring. Thus, a periodic change of the sensor patch location is required in clinical use to avoid skin burning[27] To mitigate this risk, studies have shown that using the diffusion rate of CO$_2$, rather than the equilibrating concentration of CO$_2$, as an indicator to determine the partial pressure of transcutaneous CO$_2$ can avoid skin heating in PtcCO$_2$ monitoring. [28], [29] Though promising results such as trends in CO$_2$ concentration with varying levels of activity of the subject have been demonstrated, bench-top bulky NDIR sensors are still adopted in these systems. These systems also require using pure N$_2$ to periodically purge the dead space in the sensing chamber, making them not compatible with the wearable sensing platform.

In this research, we have developed a miniaturized nondispersive infrared (NDIR) sensor-based wearable wristband device for continuously and noninvasively monitoring of transcutaneous blood CO$_2$. This miniaturized NDIR sensor is featured by its accuracy, longevity, robustness, and low-power consumption. We have also developed a hydrophobic

membrane with high CO_2 permeability to mitigate the humidity interference on the performance of the NDIR CO_2 sensor. By using the diffusion rate-based detection principle for signal processing, the wristband achieves reliable and continuous transcutaneous blood CO_2 tracking without skin heating. The performance of the NDIR CO_2 sensor-based wristband has been validated against end-tidal CO_2 monitor by simultaneously monitoring the arterial blood CO_2 change of a subject over various activities throughout the day.

II.   Materials and Methods

A.   Integrating Miniaturized NDIR Sensor to Wristband

Nondispersive infrared (NDIR) sensor is the most common kind of CO_2 sensor. It detects CO_2 by measuring the IR absorption fingerprint of CO_2 molecules at the wavelength of 4.26 microns and using Beer-Lambert's law to quantify the CO_2 concentration in the gas sample. Tremendous efforts have been spent to miniaturize the size of the NDIR CO_2 sensors in the past decades. With the advances of optics and waveguide design, longer optical light path has been dramatically folded, allowing the production of miniature NDIR CO_2 sensors with higher sensitivity and reliability. We have used a Cozir NDIR CO_2 sensor to build the wearable transcutaneous CO_2 wristband (Fig. 1(c)). The Cozir NDIR CO_2 sensor is based on solid-state LED technology and featured coin-sized form factor (ø20.9mm × 18.1mm), light weight (4g), low power consumption (3.35mW @ 3.3V), fast response time (30s), high accuracy (±70ppm), wide dynamic range (0–5%), and long lifetime (>15 years). All these features make it very suitable for wearable sensing platform. This sensor has been used for healthcare, safety, and aerospace etc. The sensor has a built-in auto-calibration system, which uses the default fresh air CO_2 concentration of 400ppm to calibrate the sensor. The sensor can constantly send streaming measurement data twice per second via its UART interface. Because of the high accuracy and real-time sensing capability, the Cozir NDIR CO_2 sensor can be directly integrated into an enclosed chamber on the wristband for continuous transcutaneous CO_2 monitoring without implementing any active gas sampling components to the system, as shown in Fig. 1.

The integrated wristband for continuous transcutaneous CO_2 monitoring is illustrated in Fig. 1. The wristband consists of a 3D printed plastic body that accommodates the Cozir NDIR CO_2 sensor. The CO_2 sensor is exposed to a miniaturized gas chamber (volume of 1.0 ml), where the transcutaneous CO_2 released from the skin can diffuse directly in and accumulate in a fixed space. An O-ring placed over the gas chamber acts as a cushion between the watch and the skin, which also provides air-tight sealing to avoid any gas leakage from or into the ambient air.

The Cozir NDIR CO_2 sensor was mounted on a circuit board that hosted UART connectivity to report the sensor data. The sensor was connected to a Windows PC using UART-USB connector to power the sensor circuit. The "GasLab" software was used to collect, view and save the sensor data. The software also provided an interface to calibrate the sensor when necessary.

B. Using Hydrophobic Membrane to Mitigate the Humidity Interference

Transcutaneous blood gas is humid, because water molecules leave human skin through diffusion and sweating. [30], [31] Water molecules interfere non-dispersive infrared gas sensors [32] since the absorption spectrum of water shows high extinction coefficient at wavelengths close to 4.26 microns. [33] The initial tests were performed by strapping the watch to a subject's wrist. The subject was in resting condition and seated in a room with an ambient temperature of 25 °C. The wristband was worn on the same wrist for all the tests. As seen in Fig. 2, the trend in the buildup of CO_2 within the O-ring were not reproducible due to the interference of humidity and condensation from the skin.

A hydrophobic membrane could be effective to mitigate the humidity interference for NDIR CO_2 sensor for transcutaneous blood gas measurement. Hydrophobic membranes are polymers that have low permeability to water vapor. They have been widely used in electrochemical sensors [34] and colorimetric sensors [35] to repel the water molecules. But when using them for transcutaneous gas monitoring, low permeability to water, high permeability to CO_2, and hydrophobicity (contact angle to water droplets) are the important properties that need to be considered. Membranes like Polytetrafluoroethylene (Teflon) and Polydimethylsiloxane (PDMS) have better permeability to CO_2, as shown in Table I. Traditional transcutaneous gas monitors use Teflon as the hydrophobic membrane with the associated CO_2 sensors. [36], [37] Compared to PDMS, Teflon has low permeability coefficients to both H_2O and CO_2. Though highly effective in reducing the humidity effect, Teflon also decreases the sensitivity of the sensor for transcutaneous CO_2 monitoring. Fig. 3 shows the response of NDIR CO_2 sensor to transcutaneous CO_2 measured on the arm of a subject with Teflon or the PDMS membrane. It is clear that the response from the sensor with Teflon is only 1/3 the response from sensor with the PDMS membrane. Compared with the NDIR CO_2 sensor response in Fig. 2, it is evident that the sensors with hydrophobic membranes show well-behaved response curves, which reflect the mass transportation process of CO_2 molecules through the membrane. The sensing signal increases quickly at the beginning as the CO_2 molecules diffuse from the gas chamber to the sensor side due to the concentration gradient and then reach a plateau when the concentration equilibrium is established. PDMS is used in applications that require high permeability of gases, [38] which is important for fast-response sensing. Since real-time transcutaneous CO_2 monitoring requires high sensitivity and fast response time, we have chosen PDMS as the hydrophobic membrane in our wristband design.

The membrane was synthesized by using Sylgard™ 184 Silicone Elastomer Kit from Dow Corning Corporation. A petri dish with the diameter of 50mm was used and 0.9 g elastomer solution was spread across the base of the petri dish. The solution was cured at 45°C overnight to produce a membrane with a thickness of 0.15mm[43] The Teflon (Polytetrafluoroethylene) membrane (thickness 0.1 mm, size 100×100 mm) was purchased from McMaster-Carr.

C. Bench Tests

Bench tests were performed to understand the influence of the membrane on transcutaneous gases as well as the response behavior of the NDIR sensor. The offline bench test setup, as

illustrated in Fig. 4, allowed the evaluation of PDMS membrane over various concentrations of CO_2 under different conditions. The diffusion chamber on the top provided an inlet and outlet for the gas being actively pumped at a flow rate of 0.8 L min-1. A preparation phase of 5 minutes was used to allow buildup of CO_2 inside the diffusion chamber and eventually diffused towards the CO_2 sensor. The PDMS membrane was fixed on the other end of diffusion chamber. The membrane and CO_2 sensor were separated by a gap with the volume of ~1.0 ml. The chamber was purged with pure N_2 to remove any traces or residue of contaminants that remained behind between tests. The test setup was maintained at a relatively constant room temperature of 25 °C. A set of 6 different concentrations of CO_2 in the range of 0.75% to 4% were generated using a mixture of 4% CO_2 and N_2 from gas cylinders by Praxair and Matheson, respectively. The Cozir sensor was calibrated with 0% and 4% CO_2 before inserting it into the bench setup. To test the sensor response to humidity, the gases were bubbled through a bench top water bath at room temperature of 25°C, which generated humid sample gases with 85% RH. All gas samples with different CO_2 concentrations were tested back-to-back to ensure consistency between results.

D. Testing the Transcutaneous CO_2 Wristband Against End-Tidal CO_2

The subject study was approved by the Institutional Review Board of Arizona State University (IRB reference protocols # STUDY00013474). The wristwatch was evaluated against End-tidal CO_2 (EtCO2), since it was a good representative of arterial CO_2. [44]–[46] EtCO2 was measured using breath-based CO_2 monitor by VacuMed (carbon dioxide analyzer, model 17630), which was a fast-response NDIR based sensor using Nafion tubing to mitigate the humidity interference. The inlet of the CO_2 monitor was connected to a pneumotach based mask setup, which was worn by the subject for normal breathing under resting conditions. The analyzer was connected to a data acquisition system as its data logger. Then, the subject strapped on the wristband device and connected the UART-USB interface. The data loggers simultaneously collected sensor data from both the CO_2 monitor and the wristband device. The subject was asked to sit down, rest, and breathe normally during the test until the wristband reading reached a plateau. From this point, the sensor data were used to analyze the performance of wristband device.

III. Results and Discussion

A. Analytical Performance of the Transcutaneous CO_2 Wristband

As seen in Fig. 5 (a), the CO_2 response curves from the PDMS membrane covered NDIR sensor showed sharp increase first and then reach plateaus. The plateau readings were proportional to the concentrations of CO_2 diffusing into the NDIR sensor, as shown in Fig. 5 (b). The sensor response to humid CO_2 gas sample generated from water bath setup was offset from the response to dry gas sample by a linear scaling factor of 0.797, shown in Fig. 5 (c).

It was observed that the slopes at the rising stage of response curves also showed a linear correlation with the CO_2 concentration, as seen in Fig. 5 (d)–(f). This indicated that it was not necessary to wait for the sensor to reach a plateau to determine the CO_2 concentration, which could be used to reduce the response time. Considering that active sample delivery

components, e.g., pump required extra power consumption and could complicate mass transportation of transcutaneous CO_2 in the wearable device, we used the plateau response from the NDIR sensor to track the transcutaneous CO_2 when testing the sensor on subjects.

B. Validation of Transcutaneous CO₂ Wristband With End-Tidal CO2 With Human Subjects

End-tidal CO_2 (EtCO$_2$) is a reliable reference technique to validate the NDIR sensor-based wearable wristband device, since partial pressure of end-tidal CO_2 shows a strong positive correlation with arterial and transcutaneous CO_2 (TcCO$_2$). [47], [48] The end-tidal CO_2 was measured using fast-response breath analyzer (shown in Fig. 6 (a)) connected to a pneumotach based face mask and a sampling tube. The end-tidal CO_2 and wristband CO_2 signals were simultaneously monitored in real time for point-to-point comparison. As shown in Fig. 6 (b) & (c), the EtCO$_2$ was computed by selecting the concentration of CO_2 at the end of exhalation cycle right before the flip towards inhalation began. For transcutaneous CO_2 monitoring, the sensor was placed on the subject's wrist using watch straps to tightly hold on to the skin to avoid leakage. After the sensor in the wristband reaches a plateau, the EtCO$_2$ and TcCO$_2$ were monitored for another 10 minutes to ensure the subject and sensor responses were stable. The sensor signals were periodically averaged over a window of 2 minutes to remove random noise and retrieve an overall trend.

The validation test started with the subject at resting (fasting for 12 hours). The NDIR sensor reached a plateau with stable reading at resting condition. Then, the subject consumed black coffee, which caused both the end-tidal CO_2 and transcutaneous CO_2 readings to increase. The CO_2 readings peaked and then started to decrease. There was a lag time of ~5min between the transcutaneous and end-tidal CO_2, as seen in Fig. 6 (d). Between 45 and 55 min, a hyperventilation was performed by the subject. During the hyperventilation, both transcutaneous and end-tidal CO_2 quickly decreased. After the hyperventilation both transcutaneous and end-tidal CO_2 gradually increased and then reached stable readings. Following the activity change during the test, the profile of transcutaneous CO_2 corelated very well with the trend of end-tidal CO_2.

C. Use Wristband to Track Transcutaneous CO₂ During Daily Activities in Free-Living Conditions

The wristband sensor was also evaluated in a field test to track the transcutaneous CO_2 profile of a subject during daily activities in free living conditions for about 4.5 hours. Before the field test, NDIR sensor-based wearable wristband device was first calibrated against the end-tidal CO_2 using the VacuMed carbon dioxide analyzer. As suggested by the calibration curve in Fig. 7 (a), the CO_2 readings from the wristband device showed highly linear correlation with the end-tidal CO_2 readings. By using this calibration plot, the signal from the wristband device can be converted into transcutaneous CO_2 readings in partial pressure (mmHg). As shown in Fig. 7 (b), the transcutaneous CO_2 changed in accordance with the daily activities from the subject. After consuming rice, beans, and cheese for lunch, the transcutaneous CO_2 of the subject showed a quick rise. This is expected since consumption of food increases the metabolism, thus increases CO_2 release. Higher levels of CO_2 were reported after lunch, which is consistent with the trends reported in other

previous work. [28] Further consumption of black coffee caused an expected rapid increase in CO_2 as well. The result of the field test clearly demonstrated the feasibility of this NDIR sensor-based wearable wristband device for passive and unobstructive tracking of transcutaneous CO_2 in free-living conditions.

IV. Conclusion

In this research, we have developed a miniaturized nondispersive infrared (NDIR) sensor-based wearable wristband device for continuous transcutaneous CO_2 monitoring. To address the humidity interference in transcutaneous CO_2 detection, a PDMS membrane has been synthesized and integrated to the NDIR CO_2 sensor. The PDMS membrane assisted NDIR CO_2 sensor shows well-behaved response curve to humid CO_2 with its plateau reading linearly corelated with the CO_2 concentration. The NDIR sensor-based wearable wristband device has been validated against end-tidal CO_2 in human test. The profile of transcutaneous CO_2 correlated very well with the expected activities-specific end-tidal CO_2 changes over the test. The feasibility of the NDIR sensor-based wearable wristband device for passive and unobstructive tracking of transcutaneous CO_2 in free-living conditions has also been demonstrated in the field test. This research has provided a simple, cost-effective, and heating-free approach for tracking of transcutaneous CO_2 on a wearable platform. The miniaturized wristband device demonstrated in this research can be simply attached to the arm of patient with respiratory diseases, such as COVID-19, sleep apnea, and chronic obstructive pulmonary disease (COPD) for remote pulmonary gas exchange efficiency monitoring. To further enhance the long-term stability and the response time of the NDIR CO_2 sensor-based wearable wristband device, technical innovations in self-calibration, diffusion optimization, signal processing, and algorithms improvement need to be explored and evaluated. Through the integration of Bluetooth chip and battery to the sensing system, a stand-alone transcutaneous wristband can be designed for both clinical use and home use. Furthermore, the wearable transcutaneous CO_2 monitoring technology developed in this research can also be easily integrated with miniaturized and off-the-shelf pulse oximetry sensors for comprehensive assessment of arterial blood gases in routinely clinical practices.

Acknowledgment

References

[1]. Gattinoni L, Pesenti A, and Matthay M, "Understanding blood gas analysis," (in eng), Intensive Care Med, vol. 44, no. 1, pp. 91-93, 01 2018, doi: 10.1007/s00134-017-4824-y. [PubMed: 28497267]

[2]. Williams AJ, "ABC of oxygen: assessing and interpreting arterial blood gases and acid-base balance," (in eng), BMJ, vol. 317, no. 7167, pp. 1213–6, 10 1998, doi: 10.1136/bmj.317.7167.1213. [PubMed: 9794863]

[3]. Lübbers DW, "Theoretical basis of the transcutaneous blood gas measurements," (in eng), Crit Care Med, vol. 9, no. 10, pp. 721–33, 10 1981, doi: 10.1097/00003246-198110000-00011. [PubMed: 7285610]

[4]. Rithalia SV, "Developments in transcutaneous blood gas monitoring: a review," (in eng), J Med Eng Technol, vol. 15, no. 4–5, pp. 143–53, 1991 Jul-Oct 1991, doi: 10.3109/03091909109023701. [PubMed: 1800745]

[5]. Hoppenbrouwers T, Hodgman JE, Arakawa K, Durand M, and Cabal LA, "Transcutaneous oxygen and carbon dioxide during the first half year of life in premature and normal term infants," (in eng), Pediatr Res, vol. 31, no. 1, pp. 73–9, 1 1992, doi: 10.1203/00006450-199201000-00014. [PubMed: 1594335]

[6]. Okane M, Shigemitsu S, Inaba J, Koresawa M, Kubo T, and Iwasaki H, "Non-invasive continuous fetal transcutaneous pO2 and pCO2 monitoring during labor," (in eng), J Perinat Med, vol. 17, no. 6, pp. 399–410, 1989, doi: 10.1515/jpme.1989.17.6.399. [PubMed: 2517562]

[7]. Carter R and Banham SW, "Use of transcutaneous oxygen and carbon dioxide tensions for assessing indices of gas exchange during exercise testing," (in eng), Respir Med, vol. 94, no. 4, pp. 350–5, 4 2000, doi: 10.1053/rmed.1999.0714. [PubMed: 10845433]

[8]. Eberhard P, "The Design, Use, and Results of Transcutaneous Carbon Dioxide Analysis: Current and Future Directions," Anesthesia and Analgesia, vol. 105, pp. S48–S52, 12 2007, doi: 10.1213/01.ane.0000278642.16117.f8. [PubMed: 18048898]

[9]. Parker SM and Gibson GJ, "Evaluation of a transcutaneous carbon dioxide monitor ("TOSCA") in adult patients in routine respiratory practice," Respiratory Medicine, vol. 101, no. 2, pp. 261–264, 2007/2/01/ 2007, doi: 10.1016/j.rmed.2006.05.011. [PubMed: 16814537]

[10]. Kirk VG, A. C. s. H. University of Calgary, Calgary AB, Canada ED Batuyong, A. C. s. H. University of Calgary, Calgary AB, Canada, S. G. Bohn, and A. C. s. H. University of Calgary, Calgary AB, Canada, "Transcutaneous Carbon Dioxide Monitoring and Capnography During Pediatric Polysomnography," Sleep, vol. 29, no. 12, pp. 1601–1608, 2006, doi: 10.1093/sleep/29.12.1601. [PubMed: 17252891]

[11]. Storre JH, Magnet FS, Dreher M, and Windisch W, "Transcutaneous monitoring as a replacement for arterial PCO2 monitoring during nocturnal non-invasive ventilation," Respir. Med, vol. 105, no. 1, pp. 143–150, 2011/1/01/ 2011, doi: 10.1016/j.rmed.2010.10.007. [PubMed: 21030230]

[12]. Morielli A, Desjardins D, and Brouillette RT, "Transcutaneous and end-tidal carbon dioxide pressures should be measured during pediatric polysomnography," (in eng), Am Rev Respir Dis, vol. 148, no. 6 Pt 1, pp. 1599–604, 12 1993, doi: 10.1164/ajrccm/148.6_Pt_1.1599. [PubMed: 8256908]

[13]. Pradal U, Braggion C, and Mastella G, "Transcutaneous blood gas analysis during sleep and exercise in cystic fibrosis," (in eng), Pediatr Pulmonol, vol. 8, no. 3, pp. 162–7, 1990, doi: 10.1002/ppul.1950080306. [PubMed: 2349008]

[14]. Tobin MJ, "Basing Respiratory Management of COVID-19 on Physiological Principles," (in eng), Am. J. Respir. Crit. Care Med, vol. 201, no. 11, pp. 1319–1320, 6 1 2020, doi: 10.1164/rccm.202004-1076ED. [PubMed: 32281885]

[15]. Guler U, Costanzo I, and Sen D, "Emerging Blood Gas Monitors: How They Can Help With COVID-19," IEEE Solid-State Circuits Magazine, vol. 12, no. 4, pp. 33–47, 2020, doi: 10.1109/MSSC.2020.3021839.

[16]. Bezuidenhout MC et al. , "Correlating arterial blood gas, acid–base and blood pressure abnormalities with outcomes in COVID-19 intensive care patients,' Annals of Clinical Biochemistry, vol. 0, no. 0, p. 0004563220972539, doi: 10.1177/0004563220972539.

[17]. M. A. R Scientific Advisor Annette Melhedegaard Thomsen, The tcpCO2 handbook.

[18]. Franz von Wirth RG, Annette Thomsen and Jesper Bryder-Jacobsen, Radiometer Medical ApS., The tcpO2 Handbook.

[19]. Hay WW, Brockway JM, and Eyzaguirre M, "Neonatal Pulse Oximetry: Accuracy and Reliability," (in en), 1989-5-01 1989.

[20]. Jouffroy R, Jost D, and Prunet B, "Prehospital pulse oximetry: a red flag for early detection of silent hypoxemia in COVID-19 patients," (in eng), Crit Care, vol. 24, no. 1, p. 313, 06 2020, doi: 10.1186/s13054-020-03036-9. [PubMed: 32513249]

[21]. Teo J, "Early Detection of Silent Hypoxia in Covid-19 Pneumonia Using Smartphone Pulse Oximetry," (in eng), J Med Syst, vol. 44, no. 8, p. 134, 6 2020, doi: 10.1007/s10916-020-01587-6. [PubMed: 32562006]

[22]. Beran AV, Huxtable RF, and Sperling DR, "Electrochemical sensor for continuous transcutaneous PCO2 measurement," J. Appl. Physiol, vol. 41, no. 3, pp. 442–447, 1976, doi: 10.1152/jappl.1976.41.3.442. [PubMed: 965318]

[23]. van Weteringen W et al. , "Novel transcutaneous sensor combining optical tcPO2 and electrochemical tcPCO2 monitoring with reflectance pulse oximetry," Med Biol Eng Comput, vol. 58, no. 2, pp. 239–247, 2020/2/01 2020, doi: 10.1007/s11517-019-02067-x. [PubMed: 31741291]

[24]. Hwan-Joo L, Do-Eok K, Dae-Hyuk K, Seung-Ha L, and Shin-Won K, "Development of non-invasive optical transcutaneous pCO/sub 2/ gas sensor and analytic equipment," in SENSORS, 2004 IEEE, 24–27 10. 2004 2004, pp. 730–733 vol.2, doi: 10.1109/ICSENS.2004.1426271.

[25]. Vurek GG, Feustel PJ, and Severinghaus JW, "A fiber optic PCO2 sensor," (in eng), Ann Biomed Eng, vol. 11, no. 6, pp. 499–510, 1983, doi: 10.1007/BF02364081. [PubMed: 6439082]

[26]. Gehrich JL et al. , "Optical Fluorescence and Its Application to an Intravascular Blood Gas Monitoring System," IEEE Transactions on Biomedical Engineering, vol. BME-33, no. 2, pp. 117–132, 1986, doi: 10.1109/TBME.1986.325886.

[27]. Tobias JD, "Transcutaneous carbon dioxide monitoring in infants and children," (in eng), Paediatr Anaesth, vol. 19, no. 5, pp. 434–44, 5 2009, doi: 10.1111/j.1460-9592.2009.02930.x. [PubMed: 19236597]

[28]. Chatterjee M, Ge X, Kostov Y, Tolosa L, and Rao G, "A novel approach toward noninvasive monitoring of transcutaneous CO2," Med. Eng. Phys, vol. 36, no. 1, pp. 136–139, 2014/1/01/ 2014, doi: 10.1016/j.medengphy.2013.07.001. [PubMed: 23931988]

[29]. Chatterjee M et al. , "A rate-based transcutaneous CO2sensor for noninvasive respiration monitoring," Physiol. Meas, vol. 36, no. 5, pp. 883–894, 2015/4/02 2015, doi: 10.1088/0967-3334/36/5/883. [PubMed: 25832294]

[30]. BUETTNER KJ, "Diffusion of water vapor through small areas of human skin in normal environment," (in eng), J Appl Physiol, vol. 14, no. 2, pp. 259–75, 3 1959.

[31]. BREBNER DF, KERSLAKE DM, and WADDELL JL, "The diffusion of water vapour through human skin," (in eng), J Physiol, vol. 132, no. 1, pp. 225–31, 4 1956, doi: 10.1113/jphysiol.1956.sp005516. [PubMed: 13320386]

[32]. Dinh T-V, Choi I-Y, Son Y-S, and Kim J-C, "A review on non-dispersive infrared gas sensors: Improvement of sensor detection limit and interference correction," Sensors and Actuators B : Chemical, vol. 231, pp. 529–538, 2016/8/01/ 2016, doi: 10.1016/j.snb.2016.03.040.

[33]. Lee R and Kester W. "Complete Gas Sensor Circuit Using Nondispersive Infrared (NDIR)." https://www.analog.com/en/analog-dialogue/articles/complete-gas-sensor-circuit-using-nondispersive-infrared.html (accessed 9 September, 2020).

[34]. Stetter JR and Li J, "Amperometric Gas SensorsA Review," Chemical Reviews, vol. 108, no. 2, pp. 352–366, 2008/2/01 2008, doi: 10.1021/cr0681039. [PubMed: 18201108]

[35]. Li Z, Askim JR, and Suslick KS, "The Optoelectronic Nose: Colorimetric and Fluorometric Sensor Arrays," Chemical Reviews, vol. 119, no. 1, pp. 231–292, 1 2019, doi: 10.1021/acs.chemrev.8b00226. [PubMed: 30207700]

[36]. Hazenberg A, Zijlstra JG, Kerstjens HA, and Wijkstra PJ, "Validation of a transcutaneous CO2 monitor in adult patients with chronic respiratory failure," Respiration, vol. 81, no. 3, pp. 242–246, 2011. [PubMed: 21242669]

[37]. Eberhard P and Palma J-P, "Device for the combined measurement of the arterial oxygen saturation and the transcutaneous CO2 partial pressure on an ear lobe," ed: Google Patents, 2003.

[38]. J. P. M, "Membrane Gas Exchange," 2010. [Online]. Available: https://permselect.com/membranes

[39]. Alqaheem Y, Alomair A, Vinoba M, and Pérez A, "Polymeric Gas-Separation Membranes for Petroleum Refining," International Journal of Polymer Science, vol. 2017, p. 4250927, 2017/2/19 2017, doi: 10.1155/2017/4250927.

[40]. Scholes C, "Water Resistant Composite Membranes for Carbon Dioxide Separation from Methane," Applied Sciences, vol. 8, p. 829, 05/21 2018, doi: 10.3390/app8050829.

[41]. Chaudhuri RG and Paria S, "Dynamic contact angles on PTFE surface by aqueous surfactant solution in the absence and presence of electrolytes," J. Colloid Interface Sci, vol. 337, no. 2, pp. 555–562, 2009/9/15/ 2009, doi: 10.1016/j.jcis.2009.05.033. [PubMed: 19505694]

[42]. Mata A, Fleischman AJ, and Roy S, "Characterization of Polydimethylsiloxane (PDMS) Properties for Biomedical Micro/Nanosystems," Biomed. Microdevices, vol. 7, no. 4, pp. 281–293, 2005/12/01 2005, doi: 10.1007/s10544-005-6070-2. [PubMed: 16404506]

[43]. Mäki AJ, Peltokangas M, Kreutzer J, Auvinen S, and Kallio P, "Modeling carbon dioxide transport in PDMS-based microfluidic cell culture devices," Chem. Eng. Sci, vol. 137, pp. 515–524, 2015/12/01/ 2015, doi: 10.1016/j.ces.2015.06.065.

[44]. Wu CH, Chou HC, Hsieh WS, Chen WK, Huang PY, and Tsao PN, "Good estimation of arterial carbon dioxide by end-tidal carbon dioxide monitoring in the neonatal intensive care unit," Pediatric pulmonology, vol. 35, no. 4, pp. 292–295, 2003. [PubMed: 12629627]

[45]. Yosefy C, Hay E, Nasri Y, Magen E, and Reisin L, "End tidal carbon dioxide as a predictor of the arterial PCO2 in the emergency department setting," Emergency Medicine Journal, vol. 21, no. 5, pp. 557–559, 2004. [PubMed: 15333528]

[46]. Barten CW and Wang ES, "Correlation of end-tidal CO2 measurements to arterial PaCO2 in nonintubated patients," Annals of emergency medicine, vol. 23, no. 3, pp. 560–563, 1994. [PubMed: 8135434]

[47]. Wollburg E, Roth WT, and Kim S, "End-tidal versus transcutaneous measurement of PCO2 during voluntary hypo- and hyperventilation," Int. J. Psychophysiol, vol. 71, no. 2, pp. 103–108, 2009/2/01/ 2009, doi: 10.1016/j.ijpsycho.2008.07.011. [PubMed: 18706460]

[48]. Barten CW and Wang ESJ, "Correlation of end-tidal CO2 measurements to arterial Paco2 in nonintubated patients," Ann. Emergency Med, vol. 23, no. 3, pp. 560–563, 1994/3/01/ 1994, doi: 10.1016/S0196-0644(94)70078-8.
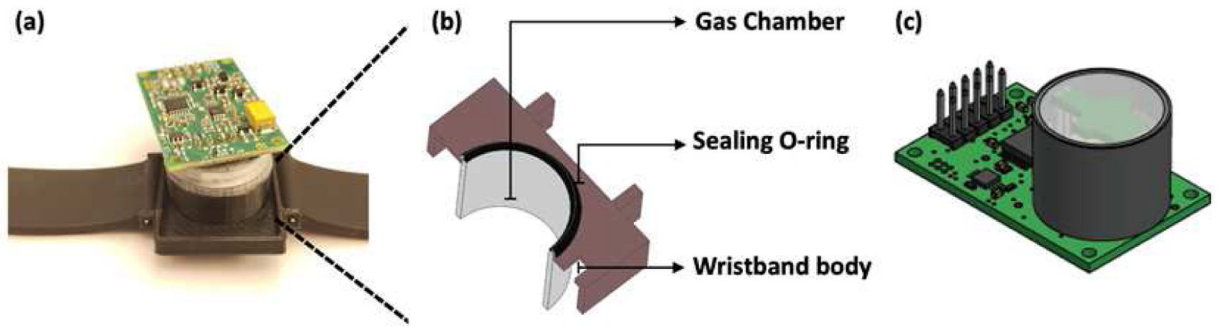
Fig. 1.
Wearable Transcutaneous CO_2 Monitor Based on Miniaturized Nondispersive Infrared Sensor. (A) Image of the integrated wristband. (B) The zoom-in shows cross-section view of the gas chamber, sealing O-ring, and wristband body. (C) Miniaturized Cozir NDIR CO_2 sensor.
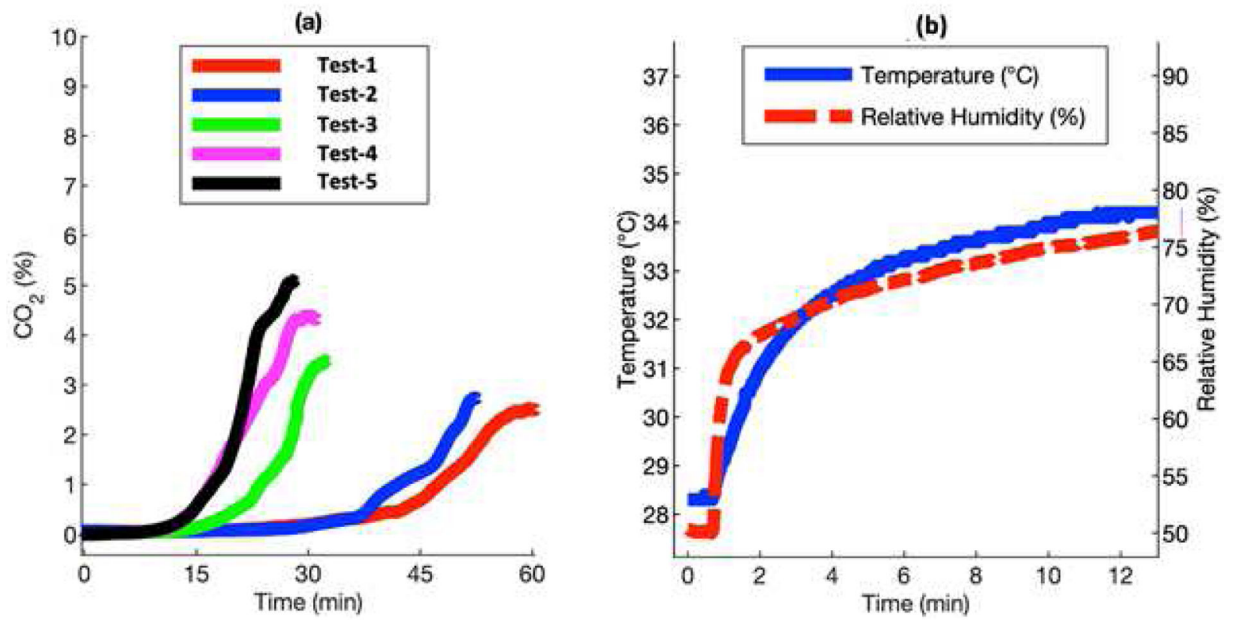
Fig. 2.
Response of Cozir NDIR CO_2 sensor to transcutaneous CO_2. (a) Measurements with interference from humidity and condensation. (b) The temperature and humidity profile of the setup when the wristband was strapped to the skin.
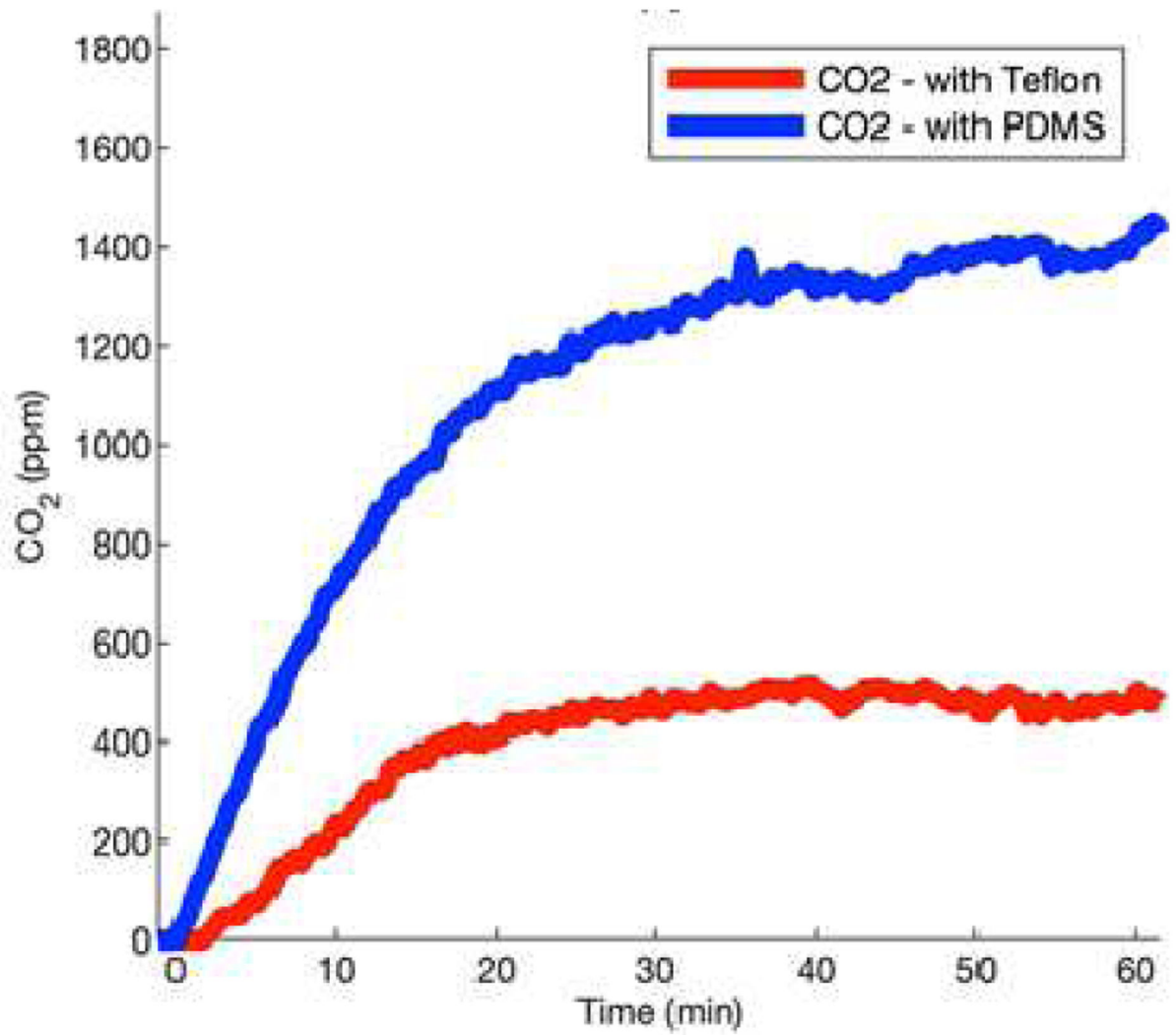
Fig. 3.
Evaluation of hydrophobic membranes for NDIR CO_2 sensing in the wristband. Response of the CO_2 sensor with the Teflon and PDMS membranes when tested transcutaneous CO_2 on the arm of a subject.
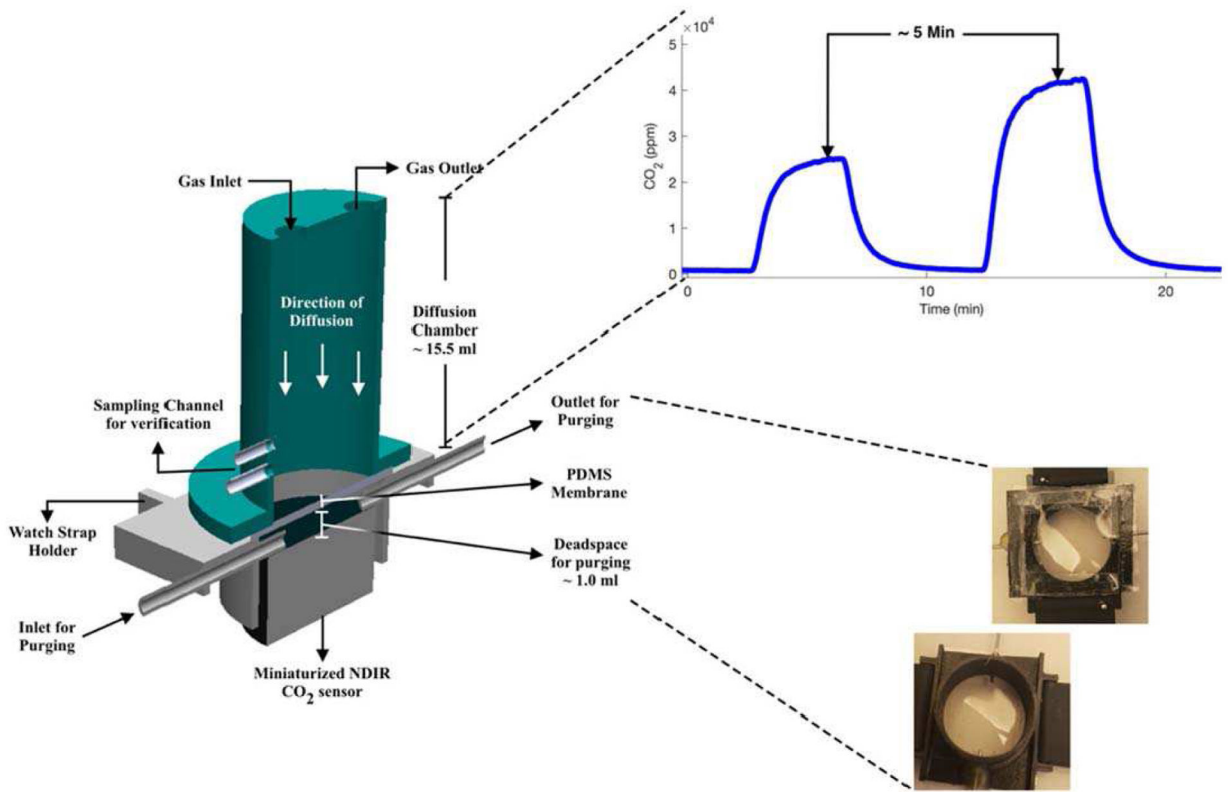
Fig. 4.
Schematic of the setup for bench tests.
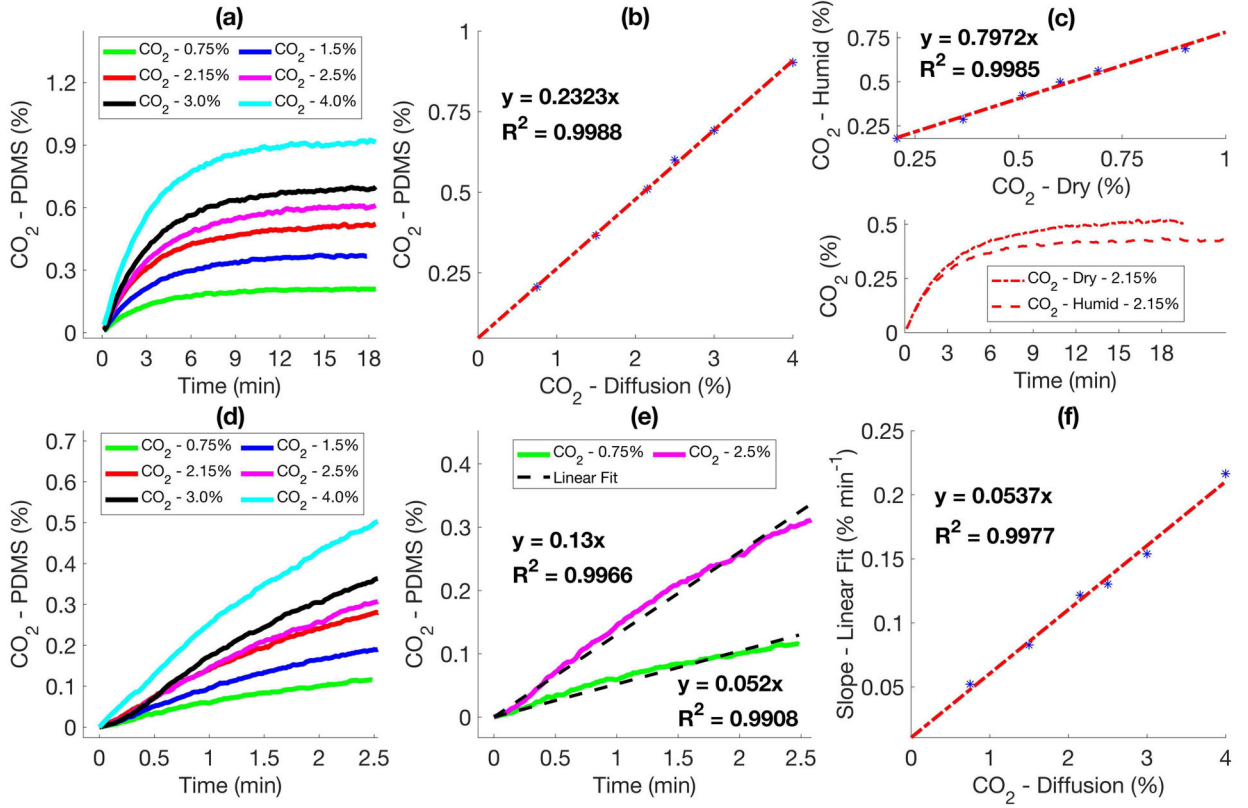
Fig. 5.
Performance of Cozir CO_2 sensor with PDMS membrane. (a) Response of the sensor for varying conc. of CO_2 pumped into the diffusion chamber. (b) Correlation between the plateau and the conc. of CO_2 shown in (a). (c) Correlation between the response of Cozir sensor to dry and humid CO_2. (d) Rise in CO_2 across the PDMS membrane after purging the sensor with N_2. (e) Linear fit of the CO_2 trends shown in (d). (f) Correlation between the slope of the linear fit and absolute concentration of diffusing CO_2.
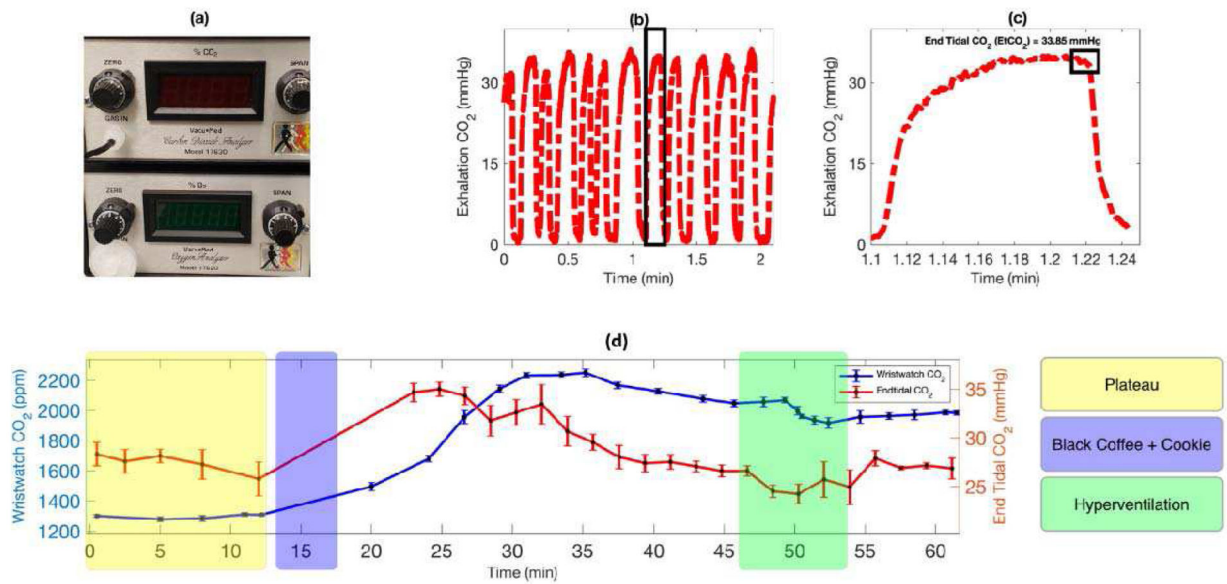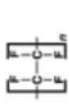
Fig. 6.

Validate the transcutaneous CO_2 wristband with end-tidal CO_2 on human subject. (a) VacuMed carbon dioxide analyzer, model 17630, is used to track end-tidal CO_2 in real time. (b) The real time profile of exhalation carbon dioxide by the subject. (c) Zoom-In plot of a single respiratory cycle with an indication of end tidal CO_2. (d) Profiles of transcutaneous and end-tidal CO_2 from a subject under various activities (i.e., baseline/plateau, consumption of black coffee and cookie, and hyperventilation).
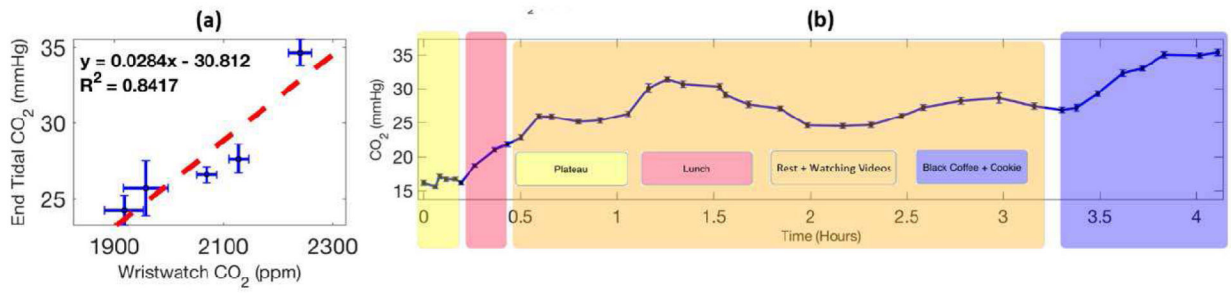
Fig. 7.
(a) Calibration of transcutaneous CO_2 wristband with end-tidal CO_2. (b) Tracking the transcutaneous CO_2 profile of a subject during daily activities in free-living conditions with the wristband device.

Author Manuscript

Author Manuscript

Author Manuscript

Author Manuscript

TABLE I

H_2O and CO_2 Permeability Coefficients Comparison Between Teflon and PDMS Membranes. [39]–[42]

Membrane			Permeability Coefficient (Barrer[*])	
Name	Structure & Appearence	Contact Angle ($°$)	H_2O	CO_2
Polytetrafluoroethylene (Teflon)		115.3	425	520
Polydimethylsiloxane (PDMS)		113.5	45,000	4000

[*]Barrer $= 10^{-10}$ cm^3 . cm/cm^2 . s . cmHg